

Photoluminescent characteristics of hafnium oxide layers activated with trivalent terbium ($\text{HfO}_2:\text{Tb}^{+3}$)

J. GUZMÁN-MENDOZA[†], D. ALBARRÁN-ARREGUÍN[†], O. ALVAREZ-FRAGOSO^{*†},
M. A. ALVAREZ-PEREZ[†], C. FALCONY[‡] and M. GARCÍA-HIPÓLITO[†]

[†]Instituto de Investigaciones en Materiales, Universidad Nacional Autónoma de México,
A.P. 70-360, Coyoacán 04510, México, D.F., Mexico

[‡]Departamento de Física, CINVESTAV-IPN, Apdo. Postal 14-740,
07000 México D.F., Mexico

(Received 1 September 2006; revised 17 November 2006; in final form 13 March 2007)

Hafnium oxide layers doped with trivalent terbium ions have been synthesized using the ultrasonic spray pyrolysis technique. Photoluminescence properties were studied as a function of growth parameters such as the substrate temperature and the terbium concentration. The films were grown starting from aqueous solution of Hafnium and Terbium chlorides. The results show that crystalline structure of $\text{HfO}_2:\text{Tb}^{+3}$ films depends on the temperature. Emission and excitation spectra were obtained for the $\text{HfO}_2:\text{Tb}^{+3}$ films using 262 nm as the excitation wavelength. All emission spectra show bands centered at 488, 542, 584 and 621 nm, which correspond to the electronic transitions: $^5\text{D}_4 \rightarrow ^7\text{F}_j$ ($j = 3, \dots, 6$) characteristic of trivalent terbium ion. The dominant emission intensity corresponds to the green color, which depend on the terbium concentration incorporated inside the host matrix.

Keywords: Photoluminescence; Spray pyrolysis; Photoluminescence hafnium oxide coatings

1. Introduction

In recent years, many investigations have been dedicated to hafnium oxide (HfO_2) compound due to its chemical and physical properties. Hafnium oxide is a high refractive index material with a wide band gap (5.68 eV) [1]. Its transparency is extended over a wide spectral range, from the ultraviolet to the mid-infrared [2]. As a result, hafnium oxide is widely used in optical coating applications [3, 4]. Furthermore, HfO_2 can be used as protective coating due to its thermal stability and hardness. In microelectronics, HfO_2 has recently received considerable attention as an alternative material for silicon oxide for its use as a high- k gate dielectric layer in metal oxide-semiconductor devices of the next generation [5, 6].

Many techniques are used to prepare hafnium oxide films; these include atomic layer deposition [8, 9] electron beam evaporation [7, 10], ion-assisted electron beam deposition [11, 12], chemical vapor deposition [13] and sol-gel [14]. However, the ultrasonic spray pyrolysis has

*Corresponding author. Tel.: +52-55-56-22-46-49; Fax: +52-55-56-16-13-71; Email: oaf@servidor.unam.mx

proved to be an efficient, low cost technique to synthesize films of metallic oxides [15]. In this work, due to the few studies existent on the luminescent properties of HfO_2 doped with rare earth ions [2, 14], we applied the ultrasonic spray pyrolysis technique to produce $\text{HfO}_2:\text{Tb}^{3+}$ luminescent layers. We explored the potential of terbium activated HfO_2 coatings to produce efficient luminescent materials that can be used for color plasma display panels, electroluminescent flat panel displays, fluorescent lamps, cathode ray tubes, scintillation devices, X-ray imaging, surface waveguide, etc.

In this paper, we reported the synthesis and characterization of photoluminescent (PL) Tb-doped HfO_2 coatings, deposited by ultrasonic spray pyrolysis technique. Also, it presented the role that it plays on some deposition parameters, such as the substrate temperature and doping concentration, in its crystalline microstructure and PL properties.

2. Experimental

Terbium-doped hafnium oxide coatings were elaborated using the ultrasonic spray pyrolysis process; this is an easy and low cost deposition technique compatible with large areas of application. This technique has been described previously [15]. The starting reagents to deposit $\text{HfO}_2:\text{Tb}^{3+}$ films were $\text{HfCl}_2 \cdot 8\text{H}_2\text{O}$ and $\text{TbCl}_3 \cdot 6\text{H}_2\text{O}$ (Aldrich Co.). The spraying solution was prepared to 0.7 M molar concentration in de-ionized water as the solvent. The doping concentrations ($\text{TbCl}_3 \cdot 6\text{H}_2\text{O}$) in the spraying solution were 2, 5, 10, 20 and 40 atomic percent (a/o), in relation to the hafnium content. Substrate temperature (T_s) during deposition was in the range from 300 °C to 550 °C and Corning 7059 glass slides were used as substrates. The carrier gas flow (air) was 8 l/min and the deposit time of the films was adjusted to 5–6 min, in order to obtain similar thickness of all the samples studied. This thickness was $\sim 10 \mu\text{m}$ as measured by a Sloan Dektak IIA profilometer. PL excitation and emission measurements were performed by using a Perkin–Elmer LS50B fluorescence spectrophotometer. All PL measurements were carried out at room temperature. The chemical composition of the films was measured by energy dispersive spectroscopy (EDS), using an Oxford Pentafet Si–Li detector integrated on a Leica–Cambridge, Scanning Electron Microscopy model stereoscan 440 (SEM) and the crystalline structure was analysed by means of X-ray diffraction (XRD), using a Siemens D-5000 diffractometer with $\text{CuK}\alpha$ radiation.

3. Results and discussion

Thickness measurements carried out showed that $\text{HfO}_2:\text{Tb}^{3+}$ films have a 10 μm thickness on an average ($\pm 0.3 \mu\text{m}$). The XRD measurements of $\text{HfO}_2:\text{Tb}^{3+}$ (5%) films as a function of the substrate temperature are shown in figure 1. For substrate temperatures lesser than 450 °C, the structure of the films is non-crystalline. At higher temperatures up to 550 °C, peaks associated with monoclinic structure appear due a better crystalline structure of the layer. Diffraction patterns show reflections centered at 24.57°, 28.34°, 31.649°, 34.318°, 34.661° and 35.435° that correspond to the diffracting planes: (1 1 0), (-1 1 1), (1 1 1), (0 0 2), (0 2 0) and (2 0 0), respectively. The strongest reflection is the (-1 1 1), indicating a preferential orientation of the crystallites (referenced JCPDS 43-1017).

The surface morphology of $\text{HfO}_2:\text{Tb}^{3+}$ films was analysed by scanning electron microscopy. The results showed that this morphology depends on the deposition temperature. Figure 2 (a,b) shows the films surface at different temperatures, a crater-like morphology (holes) exist on the surface of the film deposited at 300 °C.

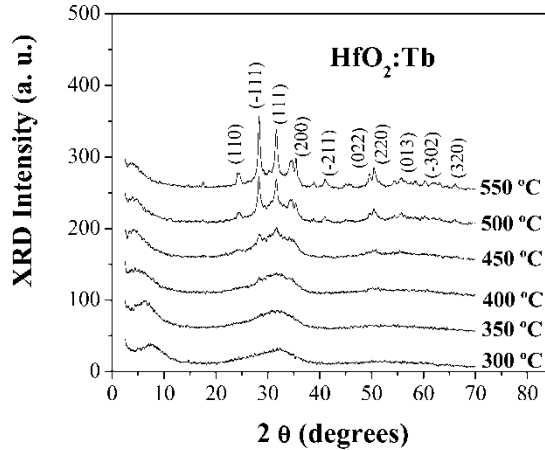


Figure 1. XRD patterns for $\text{HfO}_2:\text{Tb}^{3+}$ films at substrate temperatures of: a) 300 °C; b) 350 °C; c) 400 °C; d) 450 °C; e) 500 °C and f) 550 °C.

As the substrate temperature increases, the deposited material shows a better distribution of spherical particles with decreasing porosity. In addition, in the samples deposited at 550 °C, it is possible to distinguish between rough and continuous surface with particles that have a more spherical form (granular) with the remains of the cavernous nature of the top surface. Figure 2 (c) exhibit a SEM cross section for the $\text{HfO}_2:\text{Tb}^{3+}$ (5 a/o) film deposited at substrate temperature of 550 °C. Two kinds of structures can be observed, the first, close to the substrate, is not homogeneous, while the second, the grown, is an irregular piling up of small spheres.

Energy Dispersive Spectroscopy for different terbium concentrations keeping the substrate temperature constant (550 °C) was made to determine the chemical composition and the terbium incorporated into the films. Results are summarized in table 1. A reduction of hafnium content is observed and a terbium and chlorine increase according to the increase in activator concentration; the relative content of oxygen is maintained almost constant. The observed reduction of hafnium content presumably is due to the terbium and chlorine incorporation into the host matrix. Likewise, table 2 shows the chemicals analyses of the films prepared to different temperatures with 5 (a/o) of terbium in the initial solution. An increase in the hafnium content and a reduction of the terbium and chlorine content, as the substrate temperature increases is observed; the relative content of oxygen is maintained without remarkable variations.

At low substrate temperatures, the surface thermal energy is not enough to dissociate the initial molecules and to evaporate the solvent and the residual gases (H_2O , HCl , Cl , etc.). This inhibits the grown of the film and explains the high terbium and chloride content. The surface thermal energy increases according to the substrate temperature increase allowing it to reach a full decomposition of the initial compounds. This condition promotes the evaporation of residual products and the crystal formation of $\text{HfO}_2:\text{Tb}^{3+}$. With the crystallization, the relative hafnium and oxygen content spread to ideal stoichiometric values.

Figure 3 shows the excitation spectrum; here, it is possible to observe a band centered in 262 nm, which corresponds to the maximum value of the emission intensity—radiation with this wavelength is used to excite all $\text{HfO}_2:\text{Tb}^{3+}$ coatings in this contribution.

Figure 4 shows the PL emission spectra of $\text{HfO}_2:\text{Tb}^{3+}$ grown at 550 °C, as a function of doping concentration. Several bands center at 488, 542, 584 and 621 nm are observed, which correspond to the $^5\text{D}_4 - ^7\text{F}_6$, $^5\text{D}_4 - ^7\text{F}_5$, $^5\text{D}_4 - ^7\text{F}_4$ and $^5\text{D}_4 - ^7\text{F}_3$, characteristics transitions of terbium trivalent ion, respectively. The emission at 542 nm (green color) is the strongest.

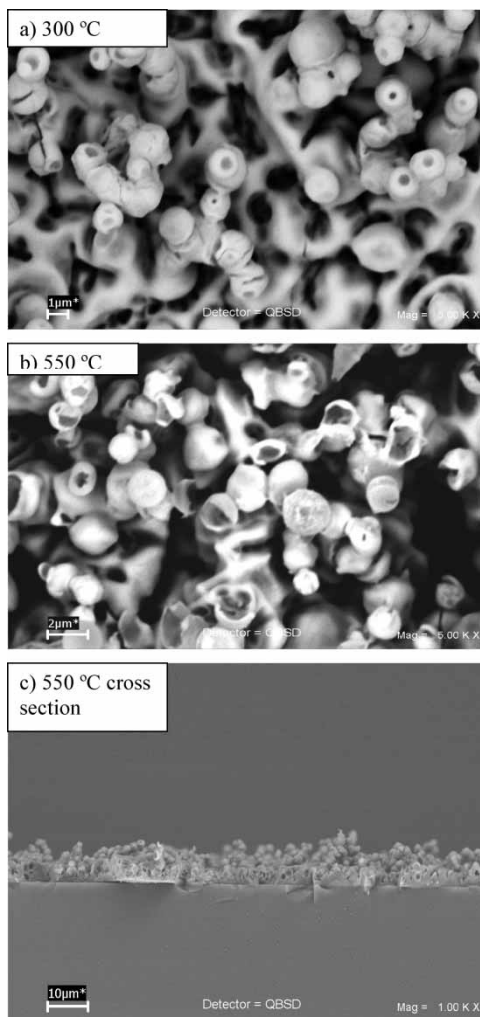


Figure 2. SEM micrographs of surface morphology of $\text{HfO}_2:\text{Tb}^{+3}$ coatings as a function of T_s : a) 300 °C; b) 550 °C; c) cross section.

Table 1. Atomic percentage of oxygen, hafnium, terbium and chlorine in $\text{HfO}_2:\text{Tb}$ films as measured by EDS deposited at different concentration of Tb (C_{Tb}) in the start solution. $T_s = 550$ °C.

C_{Tb} (a/o)	Oxygen	Hafnium	Terbium	Chlorine
0	66.74	32.62	0.00	0.64
2	68.70	29.57	0.53	1.20
5	68.03	29.30	0.95	1.72
10	67.13	27.01	2.53	3.33
20	67.90	24.46	3.63	4.01
40	68.13	21.84	4.90	5.13

As can be seen, a maximum value of the PL emission intensity for 5 a/o of TbCl_3 in the spraying solution is observed. It is also possible to note a concentration quenching for higher values than 5 a/o of TbCl_3 in the initial solution. To this respect, Dexter and Schulman [16]

Table 2. Atomic percentage of oxygen, hafnium, terbium and chlorine in $\text{HfO}_2:\text{Tb}^{+3}$ films deposited at different substrate temperatures with $C_{\text{Tb}} = 5$ a/o.

T_s (°C)	Oxygen	Hafnium	Terbium	Chlorine
300	68.43	23.58	3.42	4.57
350	67.86	25.22	2.84	4.08
400	68.29	26.20	2.20	3.31
450	68.11	27.13	1.87	2.89
500	67.87	28.84	1.19	2.10
550	68.03	29.30	0.95	1.72

have suggested that at high impurities concentration, the energy can migrate from one luminescent center to another and reach a sink, from which non-radiative processes can dissipate this energy. In this case, as the terbium content is increased in the host crystalline lattice, a resonant energy transfer effect between these ions is favored. Then, the aggregation of activators at high concentration may change some activators to quenchers and induce the quenching effect. This concentration quenching will not appear at low concentrations because the average distance between activators is so large that the migration is prevented, thus the killers are not reached [17].

The emission intensity for Tb (5% optimum doping concentration), as a function of the deposition temperature, is showed in the figure 5. The PL emission intensity always rises in accordance with the temperature increase. A better crystallization of the films as the temperature rises and a reduction of the chlorine content are probably responsible for this behavior. Both effects produce a better distribution and incorporation of the Tb ions into the host crystalline matrix, given as a result of an increment in the PL emission intensity, without any observable saturation effect of the PL emission intensity. An attempt to deposit films at substrate temperature higher than 550 °C (600 °C) was made. The obtained material was powdery, porous, not-adherent to the substrate and did not constitute a solid film.

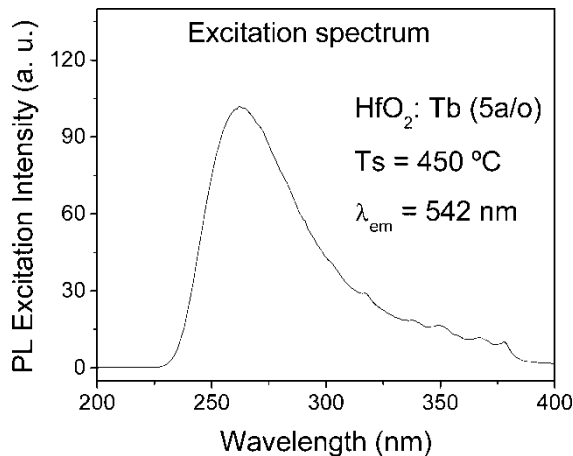


Figure 3. Excitation spectrum for $\text{HfO}_2:\text{Tb}^{+3}$ (5 a/o) films deposited at 550 °C.

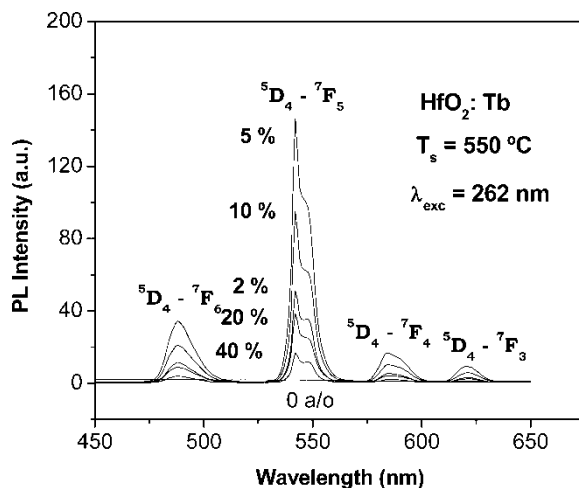


Figure 4. Typical PL spectra for $\text{HfO}_2:\text{Tb}^{+3}$ films deposited at $550\text{ }^\circ\text{C}$, as a function of terbium concentrations in the start solutions.

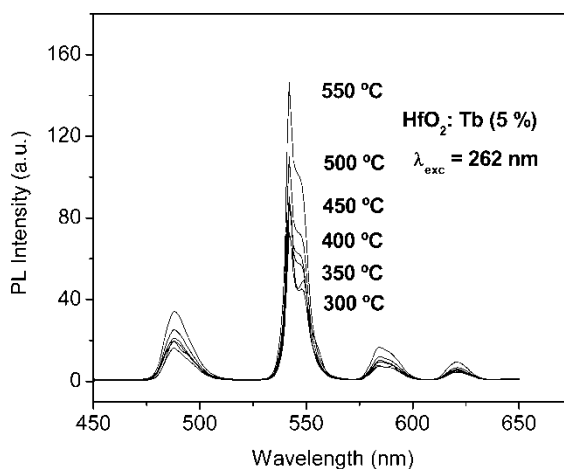


Figure 5. Substrate temperature dependence of PL emission intensity of $\text{HfO}_2:\text{Tb}^{+3}$ coatings for the optimum Tb (5 a/o) concentration.

4. Conclusions

Hafnium oxide thin films doped with terbium ions were prepared by spray pyrolysis technique. The layer thickness shows a high deposition rate of up to $2\text{ }\mu\text{m}/\text{min}$. SEM micrographs showed rough and crater-like surface with spherical particles. Their surface features depended on the substrate temperature. XRD measurements show that their crystallinity depended on the substrate temperature. At low substrate temperature, the layers are amorphous, while at high temperatures, the layers became crystalline with monoclinic phase structure. The luminescent emission of Tb doped hafnium oxide films is characteristic for the Tb^{+3} ion transitions between the levels $^5\text{D}_4 - ^7\text{F}_6$, $^5\text{D}_4 - ^7\text{F}_5$, $^5\text{D}_4 - ^7\text{F}_4$ and $^5\text{D}_4 - ^7\text{F}_3$. It was observed that concentration–quenching effect happens, if the activator concentration increases above the optimum doping concentration of 5% Tb in the start solution. A systematic increase of the PL emission intensity as the substrate temperature rises was observed without any detected saturation effect at these

used substrate temperatures. It was also confirmed that hafnium oxide is an adequate host matrix for rare earth ions as active centers to cause luminescent emissions.

Acknowledgements

The authors would like to thank to Leticia Baños, M.A. Canseco, M. Guerrero-Cruz, J. García-Coronel and Raúl Reyes for their technical support.

References

- [1] M. Balog, M. Schieber, M. Michman *et al.*, *Thin Solid Films* **41** 247 (1977).
- [2] M. Villanueva-Ibañez, C. Le Luyer, O. Marty *et al.*, *Opt. Mat.* **24** 51 (2003).
- [3] T. Mori, M. Fujiwara, R.R. Manory *et al.*, *Surf. Coat. Technol.* **169–170** 528 (2003).
- [4] M. Alvisi, S. Scaglione, S. Martelli *et al.*, *Thin Solid Films* **354** 19 (1999).
- [5] S.J. Wang, P.C. Lim, A.C.H. Huan *et al.*, *Appl. Phys. Lett.* **82** 2047 (2003).
- [6] M.J. Biercuk, D.J. Monsma, M. Marcus *et al.*, *Appl. Phys. Lett.* **83** 2405 (2003).
- [7] P.S. Lysaght, B. Foran, G. Bersuker *et al.*, *Appl. Phys. Lett.* **82** 1266 (2003).
- [8] M.Y. Ho, H. Gong, G.D. Wilk, B.W. Busch *et al.*, *J. Appl. Phys.* **93** 1477 (2003).
- [9] R. Chow, S. Falabella, G.E. Loomis *et al.*, *Appl. Opt.* **32** 5567 (1993).
- [10] M.F. Al-Kuhaili, S.M.A. Durrani and E.E. Khawaja, *J. Phys. D: Appl. Phys.* **37** 1254 (2004).
- [11] J.P. Lehan, Y. Mao, B.G. Bovard and H.A. Macleod, *Thin Solid Films*, **203** 227 (1991).
- [12] M. Gilo and N. Croitoru, *Thin Solid Films* **350** 203 (1999).
- [13] P. Baumeister and O. Arnon, *Appl. Opt.* **16** 439 (1977).
- [14] M. Villanueva-Ibañez, C. Le Luyer, C. Dujardin *et al.*, *Mat. Sci. Eng. B* **105** 12 (2003).
- [15] M. Langlet and J.C. Joubert, in *Chemistry of Advanced Materials*, edited by C.N.R. Rao (Blackwell Science, Oxford, UK 1993, p. 55).
- [16] D.L. Dexter and J.H. Schulman, *J. Chem. Phys.* **22** 1063 (1954).
- [17] G. Blasse and B.C. Grabmaier, *Lumin. Mat.* (Springer-Verlag, Berlin, 1994).

Copyright of *Radiation Effects & Defects in Solids* is the property of Taylor & Francis Ltd and its content may not be copied or emailed to multiple sites or posted to a listserv without the copyright holder's express written permission. However, users may print, download, or email articles for individual use.